Radio continuum observations of the spiral galaxies NGC 2841, NGC 5055, and NGC 7331

Hummel, E.; Bosma, A.

Published in:
The Astronomical Journal

DOI:
10.1086/113099

THE ASTRONOMICAL JOURNAL VOLUME 87, NUMBER 2 FEBRUARY 1982

RADIO CONTINUUM OBSERVATIONS OF THE SPIRAL GALAXIES NGC 2841, NGC 5055, AND NGC 7331

E. HUMMEL
Kapteyn Astronomical Institute, University of Groningen, Groningen, The Netherlands
and The University of New Mexico, Department of Physics and Astronomy, Albuquerque, New Mexico 87131

A. BOSMA
Kapteyn Astronomical Institute, University of Groningen, Groningen, The Netherlands
and Columbia University, Department of Astronomy, New York, New York 10027
Received 6 July 1981; revised 13 October 1981

ABSTRACT

The radio continuum emission of the nearby spiral galaxies NGC 2841, 5055, and 7331 has been mapped with the Westerbork Synthesis Radio Telescope at wavelengths of 50 and 21 cm. The radio continuum emission is distributed similarly to the light distribution but is not as flattened as the neutral hydrogen distribution. The spectral index distribution shows a general steepening of the radio spectrum toward the edge of the galaxies. This cannot be explained by the influence of the thermal emission alone but requires energy losses of the relativistic electrons which diffuse in both the radial and the z direction.

I. INTRODUCTION

We report here on radio continuum observations at 21 and 50 cm with the Westerbork Synthesis Radio Telescope (WSRT) of the spiral galaxies NGC 2841, 5055, and 7331. The observations were carried out in order to determine the distributon of the radio continuum emission and of the spectral index. These distributions are known in detail only for a few galaxies (cf. van der Kruit 1978), which are almost exclusively spirals with a rather strong emission from the disk component.

The radial distribution of the radio emission in the best-studied cases, NGC 5194 (M51) and NGC 6946, is roughly similar to the radial distribution of light (Allen 1975; van der Kruit 1977; van der Kruit *et al.* 1977). It is suggested that this is due to the similarity of the relativistic electron source distribution and the light distribution. The radial distribution of the spectral index shows a steepening of the radio spectrum with increasing radius, which is explained either by energy losses of the relativistic electrons (Segalovitz 1977) or by having a decreasing fraction of thermal emission with radius (van der Kruit 1977). In the latter model it is predicted that at high frequencies the thermal emission will dominate the total radio continuum emission. Recent high-frequency measurements of M51 and NGC 6946 by Klein and Emerson (1981) are not in accord with the predictions of van der Kruit's models and hence cast doubt on his explanation of the steepening of the spectral index with radius.

The galaxies discussed in this paper have weak to moderately strong disk emission (Hummel 1980, 1981) and none of them has well developed optical spiral arms. In these respects they are quite different from the well studied spirals M51 and NGC 6946, which have strong disk emission and well developed arms. In addition, for all three galaxies high-frequency flux density measurements are available and this will enable us to take into account a possible thermal contribution in the interpretation of the spectral index distribution. Table I gives some relevant optical parameters for NGC 2841, 5055, and 7331.

In Sec. II we discuss the observations and reduction, in Sec. III the results, and in Sec. IV we briefly discuss the results.

II. OBSERVATIONS AND REDUCTION

The radio continuum emission of the galaxies NGC 2841, 5055, and 7331 was observed with the WSRT at 610 and 1410 MHz. The telescope and its principles of observation are described by Baars and Hooghoudt (1974), Casse and Muller (1974), and Hogböm and Brouw (1974). In Table II we give the main characteristics of the observations. The data obtained have been calibrated and Fourier transformed according to the standard procedures described by Brouw (1971) and van Someren Gréve (1974). Further data processing has been performed by the interactive computer system described by Ekers *et al.* (1973). The 1410-MHz continuum maps of NGC 5055 and NGC 7331 were obtained from neutral hydrogen observations which are presented elsewhere (Bosma 1978); the 1410-MHz map of NGC 2841 was obtained with the standard continuum receiver.

All the maps, in particular those of 610 MHz, contain, in addition to the emission of the galaxy, a large number of discrete background sources. These sources and their instrumental responses were subtracted from the maps. This was done for field sources down to a flux density twice the rms noise level and in an area centered on the galaxy. A few sources too close to the galaxies

TABLE I. Optical parameters.

	NGC 2841	NGC 5055	NGC 7331
Right ascension	$9^h18^m35^s.0$	$13^h13^m35^s.1$	$22^h34^m47^s.2$
Declination	51°11′20″	42°17′48″	34°09′31″
Hubble type	Sb	Sbc	Sbc
B_T^0	9.58	8.93	9.51
Holmberg size	11′.3×5′.7	16′.0×10′.1	13′.5×7′.0
Position angle	148°	105°	171°
Inclination	68°	55°	75°
Distance (Mpc)	6	5	11
kpc/arcmin	1.74	1.45	3.20

Reference source for parameters

Optical position, Gallouet *et al.* (1973); Hubble type and blue magnitude (B_T^0), de Vaucouleurs *et al.* (1976); Holmberg size, Holmberg (1958); position angle, Nilson (1973); inclination, Bosma (1978); distances are derived from radial velocities (de Vaucouleurs *et al.* 1976) using $H = 100$ km s^{-1} Mpc^{-1}.

were not subtracted.

For a proper comparison of the 610- and 1410-MHz continuum maps of a galaxy, and for the construction of a spectral index map, it is essential that the same kind of structure is observed within the beam. Therefore the 610- and 1410-MHz maps have to be transformed to exactly the same beam. The 1410-MHz maps were smoothed to the same beam as the corresponding 610-MHz map and both maps were "cleaned" (Högbom 1974; Schwarz 1978) and restored with a Gaussian beam having the same half-power width in both cases. These half-power widths are given in Table II.

After the "cleaning" operation, we calculated the mean and rms noise level (see Table II) for an area away from the galaxy and adjusted the base level of the maps to zero if necessary. The maps were corrected for the primary beam attenuation of the telescopes and each pair of maps was interpolated onto the same grid before a map of the spectral index was calculated.

III. RESULTS

a) NGC 2841

A full-resolution 1410-MHz continuum observation of this galaxy has been carried out with the standard 1410-MHz continuum receiver. The final map, superimposed on an optical photograph, is presented in Fig. 1. The half-power beamwidth is 25″.4×32″.7. The position of the nucleus derived by Gallouet *et al.* (1973) from the Palomar Sky Survey prints is indicated by a cross. There is a discrepancy of 14″ between this optical position and the position of the peak of the radio emission from the galaxy. Comparison with a short-exposure photograph (Morgan 1958) shows a positional coincidence of the radio peak and the optical nucleus. The radio peak also coincides with the kinematic center as deduced from neutral hydrogen measurements (Bosma 1978). The discrepancy with the Gallouet *et al.* position is probably due to absorption effects which cause a shift

TABLE II. Observing parameters.

	NGC 2841		NGC 5055		NGC 7331	
Frequency (MHz)	1410	610	1417	610	1417	610
Date of observation	Dec. 1976	Sep. 1973 Oct. 1976 Feb. 1977	Oct. 1974 Mar. 1975	Jul. 1976 Aug. 1976	Mar. 1975 Apr. 1976	Aug. 1973 Nov. 1973
Field center:						
R.A. (h m s)	9 30 00	9 30 00	13 13 35	13 13 35	22 34 47	22 34 12
Dec. (° ′ ″)	51 12 00	51 21 00	42 17 48	42 17 48	34 9 31	33 54 00
Spacings:						
shortest (m)	36	36	36	36	36	54
longest (m)	1404	1440	720	1440	1440	1458
increment (m)	72	36	36	36	72	36
Total observing time (hrs)	1×12	2×12	—	2×12	—	2×12
Synthesized beam (arcsec)	25.4×32.7	58.7×75.4	48.9×73.4	57.1×86.3	25.2×44.9	56.9×100.7
Radius first grating ring (arcmin)	10×13	47×60	20×30	47×70	10×18	47×84
rms noise[a] (mJy/beam)	0.5 (1.0)	1.6	1.2	1.4	(0.7)	1.9
Gaussian beam (arcsec)	60×76		58×87		57×101	
Missing large-scale structure (arcmin)[b]	9×11	21×27	9×14	21×32	9×16	14×25

[a]In parentheses: after smoothing to the 610-MHz beam.
[b]For structure greater than given values, visibility is less than 0.5 (assuming Gaussian distribution).

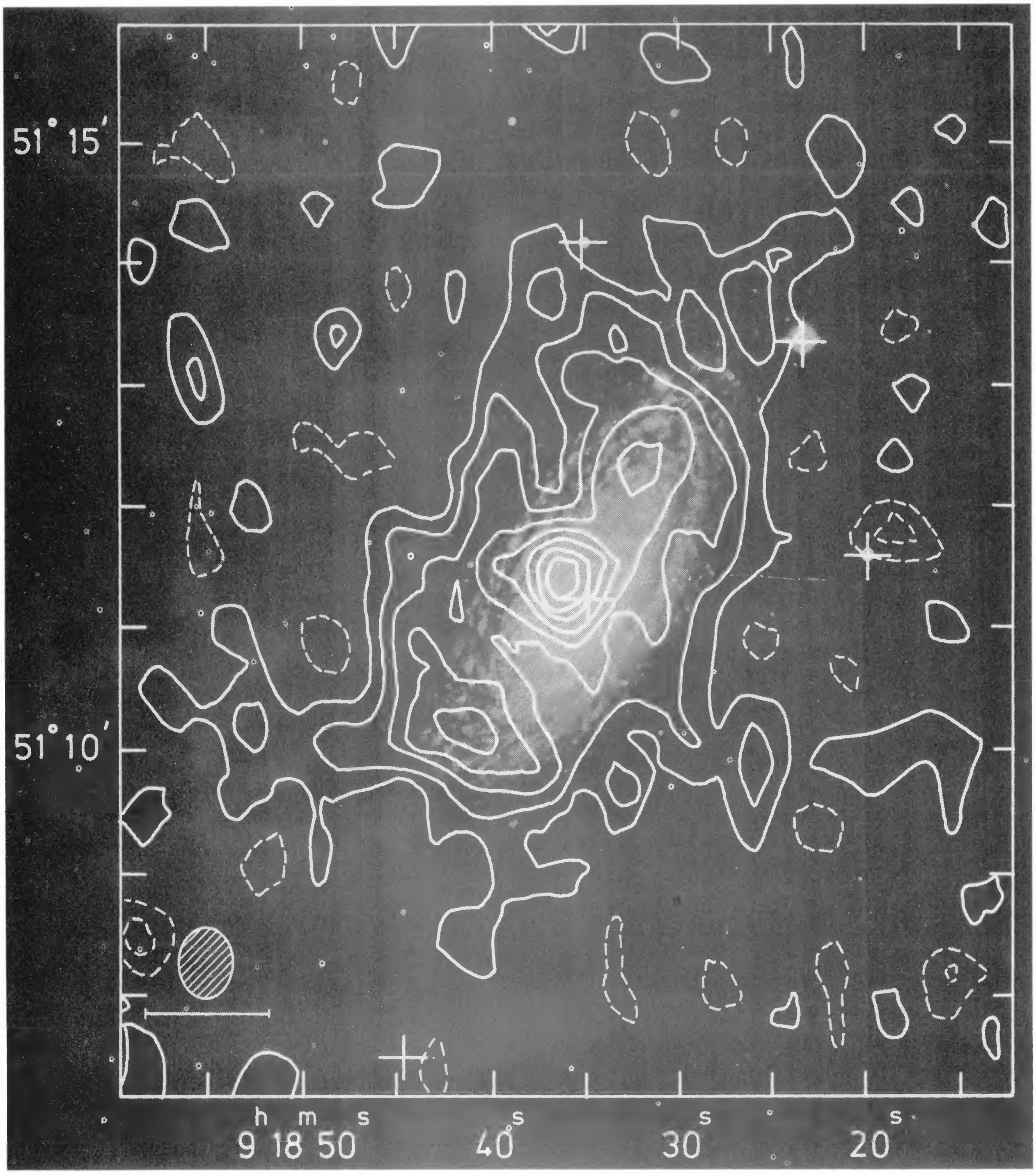

FIG. 1. The full-resolution 21-cm radio continuum map of NGC 2841 superimposed on an optical photograph. The cross indicates the optical center as given by Gallouet *et al.* (1973). The HPBW is given by the hatched ellipse; the bar has a length of 1 arcmin. The contours are from − 1.0 to 4.0 in steps of 0.5 mJy/beam. The rms noise is 0.5 mJy/beam.

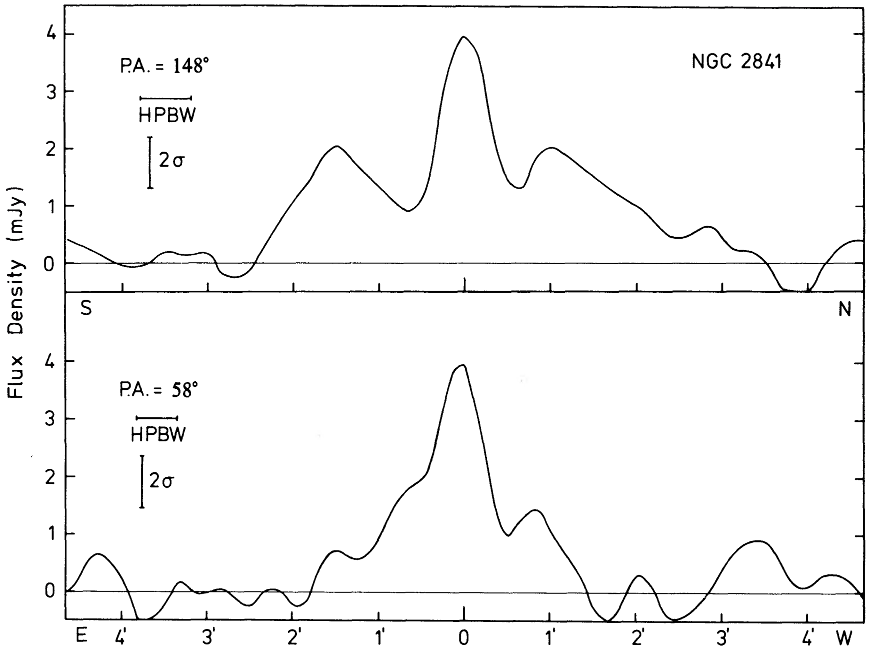

FIG. 2. The radio continuum brightness distributions at 21 cm at position angles 148° and 58° through the radio center of NGC 2841.

of the apparent centroid of the light distribution to the western edge of the galaxy image at longer exposures. In Fig. 2 we show the 1410-MHz brightness distributions along the major and minor axis of the galaxy. From these we estimate the flux density of the central source to be 3.0 ± 0.5 mJy. This source is slightly resolved; its position is R.A. $= 9^h18^m36^s\!.1 \pm 0^s\!.12$, $\delta = 51°11'26''\!.0 \pm 0''\!.5$ (1950). The peaks to the north and south of the central source may be due to an enhancement of the general disk emission by a spiral arm component. The east-west feature in the southern part is probably not related to the galaxy and must possibly be ascribed to an instrumental effect.

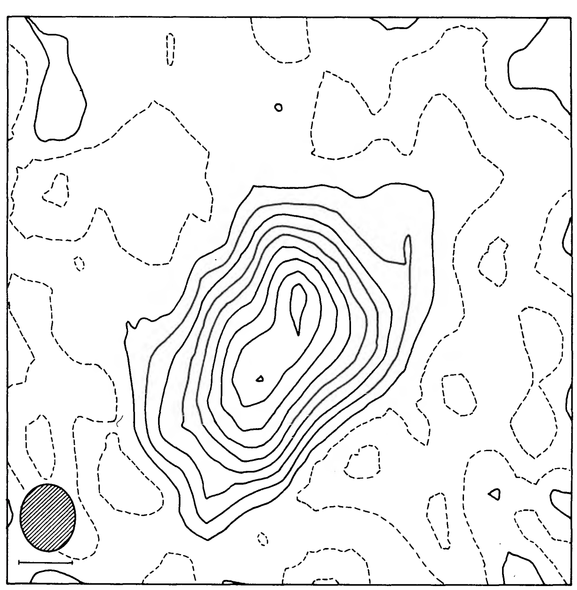

FIG. 3. The 50-cm map of NGC 2841. It is centered at R.A. $= 9^h18^m32^s$, $\delta = 51°12'15''$ and the bar is 1'. The HPBW is $60'' \times 76''$ and the rms noise is 1.6 mJy/beam. The contour interval is 2.5 mJy/beam starting at -2.5 mJy/beam.

Figure 3 shows the cleaned 610-MHz map. The resolution of this map is $60'' \times 76''$. There is an uncorrectable distortion running at a position angle of $\sim 30°$ through the northern part of the galaxy. This distortion arises from grating responses of a point source at R.A. $= 9^h13^m29^s\!.70 \pm 0^s\!.12$, $\delta = 51°25'38''\!.7 \pm 0''\!.5$ (1950) with a flux density of 460 ± 20 mJy. We estimate an uncertainty of 2 mJy in the contour levels of the 610-MHz map at the position of the distortion. At 610 MHz with our resolution there is no evidence for the presence of a central source and the emission peaks north of the 1410-MHz central source; this may be due to the abovementioned distortion.

The total flux densities at 610 and 1410 MHz were obtained by integrating over an area comparable to those of Figs. 1 and 3. These flux densities are given in Table III where we also give the deconvolved sizes along the major and minor axis at a brightness level corresponding to 10% of the peak brightness. In Fig. 4 we show the total flux density as a function of frequency. The spectrum can be fitted by a power law and the spectral index* is $\alpha = -0.78 \pm 0.05$. In view of the low signal-to-noise ratio at 1410 MHz and the distortion in our 610-MHz map, it is not possible to construct a reliable spectral index map. In the central region, where the spectral index can be determined to an accuracy of about 0.1, $\alpha \simeq -0.75$, hence not very different from the

*Spectral index α defined as $S(:)\ \nu^{\alpha}$.

TABLE III. Results.

	NGC 2841		NGC 5055		NGC 7331	
Frequency	1410	610	1417	610	1417	613
Total flux density (mJy)	75 ± 15	171 ± 35	409 ± 20	830 ± 40	486 ± 24	809 ± 40
Flux density central source (mJy)	3 ± 0.5	< 10	< 10	< 50	< 10	< 50
Deconvolved sizes (arcmin):						
major axis	6.2	7.8	6.5	6.7	4.3	6.0
minor axis	3.0	3.5	3.4	3.2	1.9	2.3
Spectral index	-0.78 ± 0.05		-0.78 ± 0.05		-0.74 ± 0.05	

total spectrum. At the position of the central source, $\alpha = -0.55$.

b) NGC 5055

A 1410-MHz continuum map of this galaxy, at a resolution of $25'' \times 37''$, has been published by van der Kruit (1973). These observations were contaminated by dc offsets in the correlators and are therefore not accurate enough to be combined with 610-MHz observations in order to calculate a spectral index map. A new 1410-MHz continuum map of this galaxy, at resolution of $49'' \times 73''$, was obtained as a by-product of 21-cm line observations discussed by Bosma (1978). After subtraction of most of the background sources, this map was smoothed and cleaned. The Gaussian beam used for the restoration had a half-power width of $58'' \times 87''$. This map is shown in Fig. 5 along with the 610-MHz map at the same resolution. Owing to the relatively low resolution, no details in the radio structure can be seen. There is no evidence for a central source. The enhancement in the northeastern part at R.A. $= 13^h14^m50^s$, $\delta = 42°18'$ has no clear counterpart on optical photographs. In van der Kruit's map it stands out as an unresolved source and we suspect it to be a background source.

The 610-MHz map is shown in Fig. 5. The background source mentioned above is now more or less merged with the emission of the galaxy. Another background source (R.A. $= 13^h13^m50^s$, $\delta = 42°12'$) with a flux density of 17 ± 2 mJy could not be removed unambiguously. Also shown is the spectral index distribution as calculated from the 610- and 1410-MHz maps. Its boundaries are determined by the 4-mJy/beam contour ($3 \times$ rms noise) of the $58'' \times 87''$ 1410-MHz map.

The total radio spectrum as shown in Fig. 4 can be fitted by a power law with $\alpha = 0.78 \pm 0.05$. At 1410 MHz there is a discrepancy between our total flux density and the values obtained by van der Kruit (1973) and Heeschen and Wade (1964). However, their values may be too high owing to the inclusion of some neutral hydrogen emission and emission from some background sources, respectively.

c) NGC 7331

A 1410-MHz continuum map of this galaxy has been published by van der Kruit (1973), but unfortunately his map is contaminated by H I line emission in the southern part of the galaxy. A new 1410-MHz continuum map has been obtained from line observations described by Bosma (1978). This map is similar to van der Kruit's map because the continuum emission is rather strong. There is no evidence for a central source. The emission is strongest on either side of the center at a distance of about 1′ from the optical center.

Figure 6 shows a smoothed and cleaned version of this map. The resolution is $57'' \times 101''$. A strong double source (van der Kruit's sources 6 and 7) has been subtracted because we believe it to be a background source. In the southern part of the galaxy there is a significant extension which is also present at 610-MHz and this rules out H I contamination. On the high-resolution 1410-MHz map the highest peak in this extension coin-

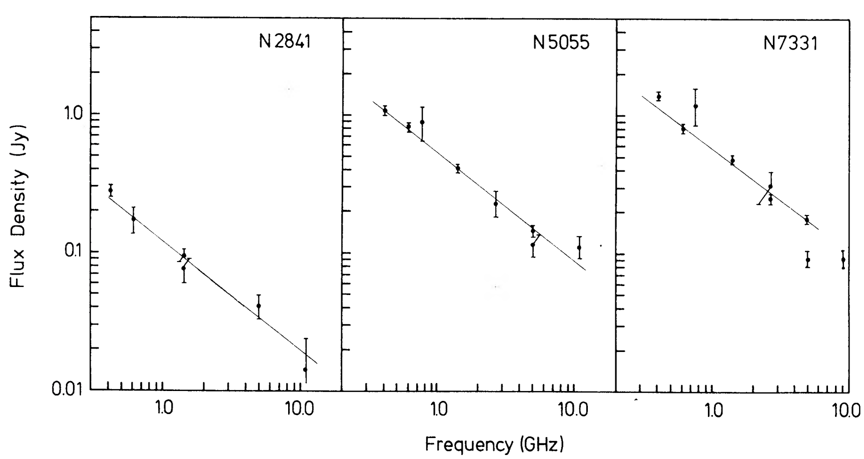

FIG. 4. The radio spectrum of the total radio emission. References: 408 MHz, Gioia and Gregorini (1980); 610 MHz, this paper; 750 MHz, de Jong (1966); 1410 MHz, this paper, for NGC 2841 also Hummel (1980); 2695 MHz, NGC 5055, Pfleiderer (1980, private communication), NGC 7331, Pfleiderer (1980, private communication) and de Jong (1967); 5000 MHz, van der Hulst (1981), NGC 5055 and NGC 7331 also Sramek (1975); 10 700 MHz, NGC 2841 and NGC 5055, Klein and Emerson (1981), NGC 7331, Israel and van der Hulst (1981).

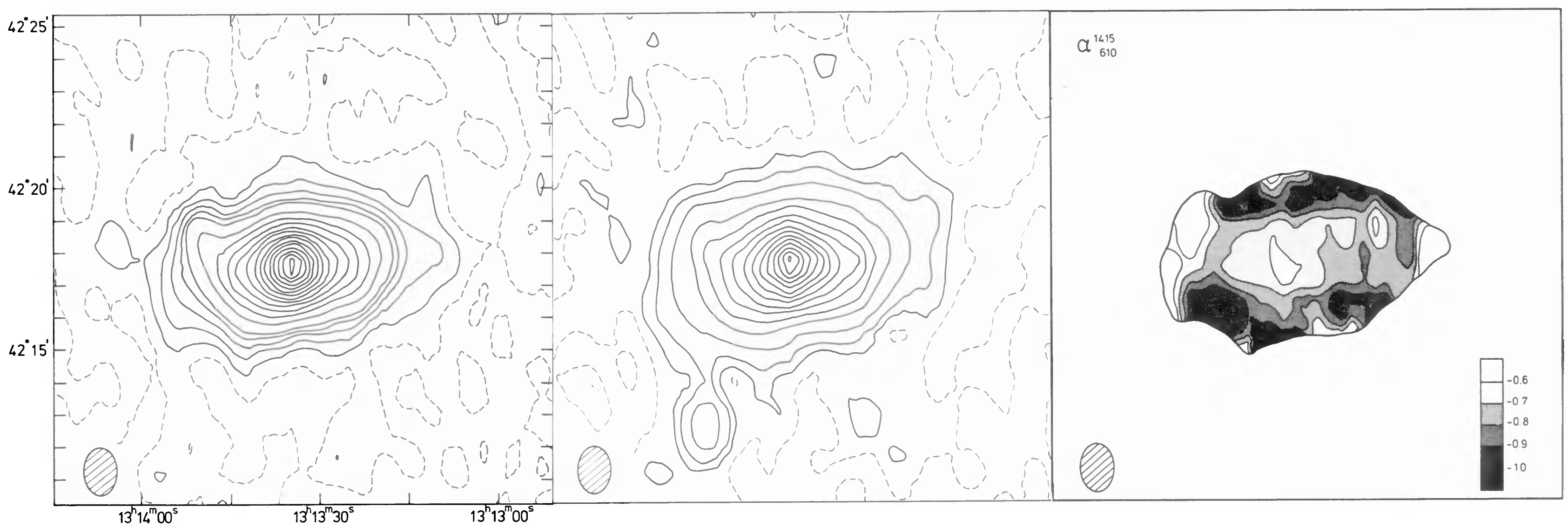

FIG. 5. The 58″ × 87″ maps at 21 and 50 cm and the spectral index map of NGC 5055. The contours at 21 cm are − 2, 0, 2, 4, 6, 8, and 10 mJy/beam and higher in steps of 5 mJy/beam. The rms noise is 1.2 mJy/beam. At 50 cm the contours are − 2.5, 0, 2.5, 5, 10, and higher in steps of 10 mJy/beam and the rms noise is 1.4 mJy/beam. The error in the spectral index map ranges from 0.1 in the central part to 0.3 at the edge which is defined by the 4 mJy/beam contour of the 58″ × 87″ 21-cm map.

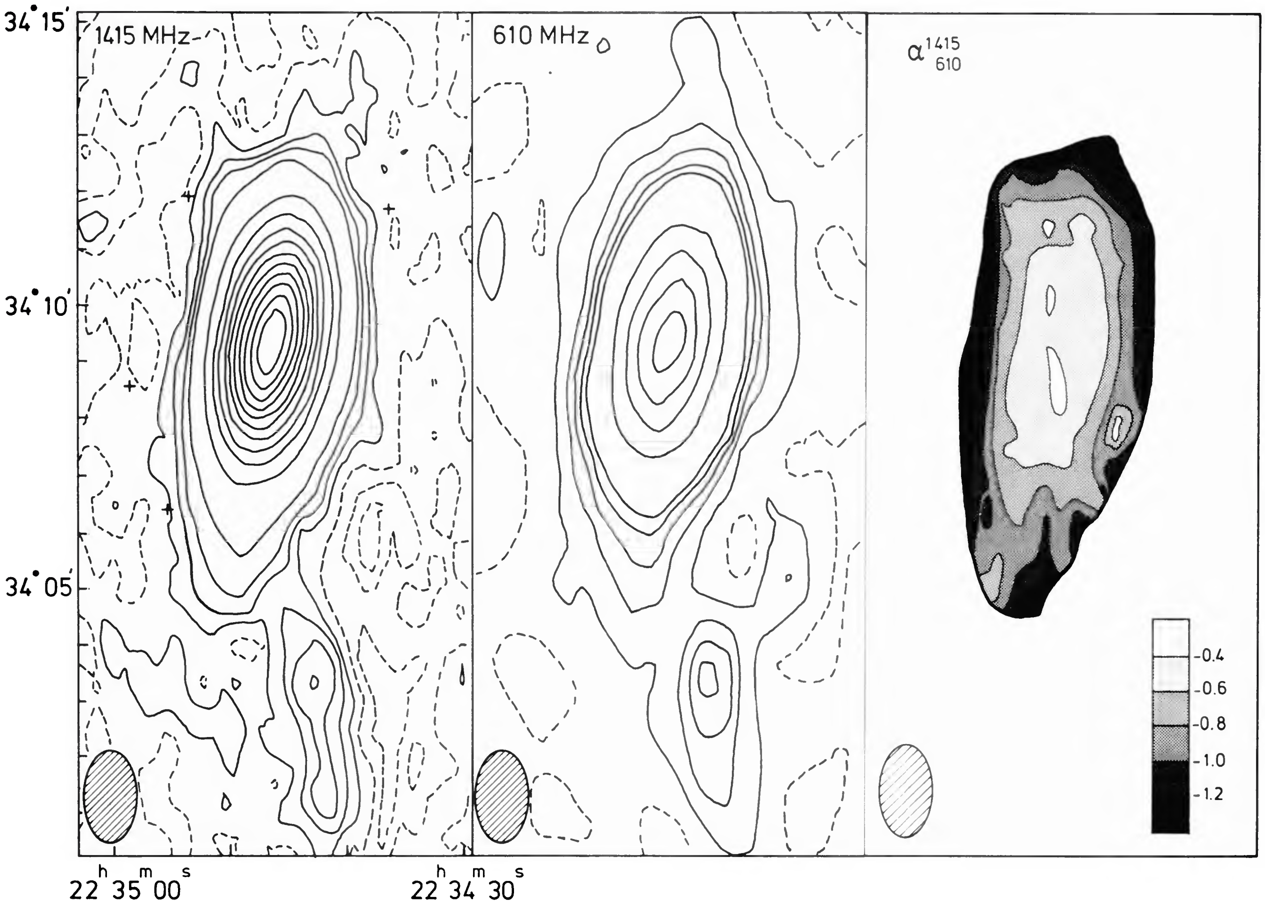

FIG. 6. The $57'' \times 101''$ maps at 21 and 50 cm and the spectral index map of NGC 7331. The contours at 21 cm are -3, 1.5, 0, 1.5, 3, 4.5, 7.5, and higher in steps of 15 mJy/beam and the rms noise is 0.7 mJy/beam. At 50 cm the contours are 0, 5, 10, 15, 20, 25, 75, 125, 175, and 225 mJy/beam and the rms noise is 1.9 mJy/beam. The error in the spectral index map ranges form 0.1 in the central part to 0.3 at the edge, which is defined by the 3-mJy/beam contour of the $57'' \times 101''$ 21-cm map.

cides with an H II complex (see also van der Kruit 1973) but it should be noted that the radio spectrum in the extension is clearly nonthermal with a spectral index of $\alpha \simeq -1.1$.

The map at 610 MHz (Fig. 6) has been obtained from a study of the Stephan's Quintet region and was kindly made available to us by Dr. R. J. Allen. We subtracted all the background sources, cleaned the map, and restored it to a resolution of $57'' \times 101''$. At this frequency the total flux density of the double source near the galaxy is 280 ± 20 mJy and the position of the centroid is R.A. $= 22^h24^m36^s.1 \pm 0.1$, $\delta = 34°5'22'' \pm 1''$. Also in this map the extension in the southern part of the galaxy is present. The total flux densities at 610 and 1410 MHz and the deconvolved sizes are given in Table III.

Figure 4 shows the radio spectrum of the total radio emission. The value at 5 GHz given by Sramek (1975) is too low because NGC 7331 is resolved by the NRAO 300-ft radio telescope. The flux densities at 408 and 750 MHz (Gioia and Gregorini 1980; de Jong 1966) are too high owing to the inclusion of the double source near the galaxy. The flux density of this background source is 280 and 143 mJy at respectively 610 and 1410 MHz and its spectral index is -0.8. When the 408- and 750-MHz flux densities are corrected for the contribution of this double source, the radio spectrum can be fitted by a power law with a spectral index of -0.74 ± 0.05. These corrections have not been applied in Fig. 4. Figure 6 shows the spectral index distribution. The boundary of this map is defined by the 3-mJy/beam contour ($\sim 4 \times$ rms noise) of the $57'' \times 101''$ 1410-MHz map. It is clear that the spectral index steepens from 0.6 ± 0.1 in the central region to -1.3 ± 0.3 in the outer parts.

d) Comments on the Results

For a fair comparison of the 610- and 1410-MHz maps it is essential that no large-scale structure is missed in one of the maps. Synthesis observations with the WSRT do not completely cover the (u,v) plane; the shortest spacings are missing which cause large-scale structures to go undetected. In Table II we list the shortest spacing used for each observation as well as the half-power sizes of a Gaussian brightness distribution having a visibility of 0.5 at this spacing. As is clear from a comparison of these sizes and the sizes at a brightness level of 10% of the peak brightness found for the galaxies (see Table III), we can be sure that no large-scale structure is missed in our observations of NGC 2841, 5055, and 7331. This is so because the cleaning procedure provides an extrapolation for the missing flux at short spacings: even if the expected visibility at 0 m is reduced somewhat, cleaning will recover the flux (Schwarz 1978). A check on this comes from an examination of the radio spectra, where most of the data are obtained from single-dish measurements. This means that e.g., the steepening of the radio spectrum towards the edges of the galaxy, is *not* due to missing structure at 1410 MHz (cf. discussion in Allen *et al.* 1978).

The main result from the 610- and 1410-MHz continuum observations of NGC 2841, 5055, and 7331 concerns the spectral index distribution in the radio disks of these galaxies. Although no reliable spectral index map of NGC 2841 could be obtained, the similarity of the spectral index in the central region (excluding the central source), where $\alpha \simeq -0.75$, and the total flux density spectrum, which has $\alpha \simeq -0.78$, show that the spectral index does not vary drastically with distance from the center of the galaxy. The two other galaxies clearly show a general steepening of the radio spectrum, especially in the direction of the minor axis (see Figs. 5 and 6). The northern and southern parts of NGC 5055 have a spectral index $\alpha \simeq -1.0$ while the central region $\alpha > -0.6$. In the direction of the major axis the spectrum steepens from > -0.6 in the center to -0.8 at 2'.5 from the center. Beyond 2'.5 the spectrum flattens again. In the eastern part this may be due to the presence of the above-mentioned background source. NGC 7331 has $\alpha \simeq -1.3$ at the edges and $\alpha \simeq -0.5$ in the central part. It should be noted, however, that especially at the edges of the galaxies, where the signal-to-noise ratio is low, the error in the spectral index can be quite large. At the edges the errors are of the order 0.3 while in the central regions they are about 0.05. The predominance of a steep spectrum at the edges of NGC 5055 and NGC 7331 clearly shows that there is a steepening of the spectrum, but the amount of that decrease in spectral index is still unclear. In NGC 5055 it is about $\Delta\alpha \simeq 0.3$ and the data for NGC 7331 suggest $\Delta\alpha \gtrsim 0.5$.

TABLE IV. Axial ratios, cosmic-ray energy density, and average magnetic field strength.

		NGC 2841	NGC 5055	NGC 7331
Axial ratio:	26.5 arcsec^{-2}	2.0	1.6	1.9
	25.0 arcsec^{-2}	2.1	1.6	2.7
	H I	2.7	1.7	3.9
	radio continuum	2.0	2.0	2.4
Radio luminosity (10^{27} erg s^{-1} Hz^{-1})		3.3	12	71
Cosmic-ray energy density (10^{-12} erg s^{-1} cm^{-3})		7.4	19	26
Average magnetic field strength (10^{-6} G)		9.0	14	17
Lifetime of relativistic electrons $t_{1/2}$ (10^{15} s)		1.1	0.6	0.4

IV. DISCUSSION

a) The Distribution of the Radio Emission

Since the relative resolution of our observations for all three galaxies is low (i.e., the radial extent of the continuum emission/beam size is of the order of 2–3), a detailed comparison of the radial distributions of radio continuum emission and light is not very meaningful. Moreover, the inclinations of these galaxies is so high that we have to consider effects due to the thickness of the disk. We will first compare the axial ratios of the light, neutral hydrogen, and the radio continuum distributions. The various axial ratios (major/minor axis diameters) are given in Table IV. The optical sizes were taken from Holmberg (1958) and de Vaucouleurs *et al.* (1976) and refer to isophote levels of 26.5 and 25 mag arcsec^{-2}, respectively. The H I axial ratio is based on the inclination found from the kinematics of the galaxies (Bosma 1978) and the radio continuum axial ratios are based on the sizes given in Table III. The optical axial ratios are essentially the same except for NGC 7331, where the light distributions become more spherical at lower intensities owing to the bulge component. In general, the H I distribution turns out to be the most flattened component; only in the case of NGC 5055 are the ratios for the various components similar.

The axial ratios suggest that the radio continuum emission is distributed like the light in the disk component. This is similar to the results found in more face-on galaxies (Allen 1975; van der Kruit *et al.* 1977). In NGC 7331 the radio emission distribution is flatter than the bulge component. If we assume that the H I distribution is flat, then the radio continuum emission of NGC 2841 and NGC 7331 has its largest extent in the direction perpendicular to the plane of the galaxies of about 4 kpc. This can be compared to the largest extents found for edge-on galaxies which range from 2 to 14 kpc (Hummel *et al.* 1982). The highest value is found for NGC 4631 (Ekers and Sancisi 1977).

In Table IV we also give the energy density of the cosmic rays and the average magnetic field strength. These are calculated assuming equipartition and that there is 100 times more energy in protons than in electrons (cf. Moffet 1975). The total radio luminosity was obtained by integrating the radio spectrum from 10^7 to 10^{10} Hz. The cosmic-ray energy densities are about 10^{-11} erg cm^{-3} and the magnetic field strength is $B \sim 10\,\mu$G. These values depend only weakly on the volume of the emission region and are averages over that volume. The equipartition values found for our Galaxy are very similar to the ones found for NGC 2841. In addition, their central complexes are rather similar. Only in our Galaxy is it possible to estimate the magnetic field strength (at least locally) without assuming equipartition. The values found (Brindle *et al.* 1978; Rockstroh and Webber 1978) do not differ significantly from the equipartition value. This strengthens our belief that the values we found for the magnetic field strengths in NGC 2841, 5055, and 7331 are correct within a factor of 2.

b) The Spectral Index Distribution

The general steepening of the radio spectrum towards the outer parts in NGC 5055 and NGC 7331 has also been observed in a number of other spiral galaxies, ranging from face-on's like NGC 6946 (van der Kruit *et al.* 1977) to edge-on's like NGC 891 (Allen *et al.* 1977). The explanation for this has been a topic for debate, in particular in the case of the face-on galaxy M51 (Segalovitz 1977; van der Kruit 1977). Two possibilities are considered:

(i) The cosmic-ray sources are widely distributed through the galactic disk and are linked to the total stellar disk population. Little diffusion takes place or the relativistic electrons escape from the disk in about 10^7 yr. The thermal emission component is distributed such that the spectral index decreases with radius on account of its presence alone. Van der Kruit (1977) claims that this model explains the observations of NGC 6946 and M51.

(ii) The cosmic-ray sources are distributed in a more complicated manner and diffusion is important. The escape time for electrons is about 3×10^7 yr and the steepening of the spectrum is basically due to energy losses (Segalovitz 1977).

For the edge-on galaxy NGC 891, Allen *et al.* (1978) suggested that the steepening of the radio spectra with increasing distance from the galactic plane could be either due to a drop of the magnetic field strength with increasing z (in that case a break in the energy spectrum is necessary) or due to a change in the energy spectrum caused by losses of the cosmic-ray electrons as they propagate away from their sources, which presumably lie in the plane. Both possibilities could be important and both are compatible with Segalovitz's assumptions.

The influence of the thermal emission on the spectral index distribution has been calculated in detail by van der Kruit *et al.* (1977) and van der Kruit (1977) in their analysis of NGC 6946 and NGC 5194 (M51). However, their prediction of the total radio emission at higher frequencies (>5 GHz) turned out to be too high when compared with the 10-GHz measurements by Klein and Emerson (1981), showing that the assumed thermal contribution at 1.4 GHz was too high and that the steepening of the radio spectrum with radius of the total emission is not due only to the thermal emission distribution. This conclusion depends on the assumption made for the nonthermal radio spectrum (a single power-law radio spectrum was assumed in the prediction). But the results obtained by Klein and Emerson (1981) and Protheroe and Wolfendale (1980) strongly suggest that the nonthermal radio spectrum (if not affected by energy losses) can be fitted by a single power law at least down to 10 GHz, and that in general at 1.4 GHz the thermal contribution is almost negligibly small ($<10\%$). An unlikely alternative is that the thermal and nonthermal component conspire to get a single power-law radio spectrum for the total emission.

The radio spectra of NGC 2841, 5055, and 7331 show that there is no obvious flattening at higher frequencies. This almost certainly rules out a significant thermal contribution at 1.4 GHz. Even if *all* the emission at 10 GHz is thermal, the thermal fraction at 1.4 GHz would be $<30\%$. More realistic limits would be $\sim 15\%$. A comparison with the 10-GHz maps given by Klein and Emerson (1981) shows that in the central regions of NGC 2841 and NGC 5055 the thermal contribution is at most 30%. For NGC 5055, this high limit for the thermal emission in the center would result in a spectral index of the nonthermal component of -0.6, still significantly higher than at a radius of 2′.5 and at the northern and southern edge. As already mentioned, in the case of NGC 2841 the signal-to-noise ratio is too low to justify an analysis of the spectral index distribution. NGC 7331 would require a thermal contribution at 1.4 GHz of $\sim 40\%$ (even $\sim 60\%$ in the central area) to get essentially the same nonthermal spectral index of -0.8 out to 2′.5. This seems to be unrealistically high in view of the Klein and Emerson (1981) and Israel and van der Hulst (1981) results.

We can conclude that in NGC 5055 and NGC 7331 the steepening of the radio spectrum is mainly due to energy losses of the relativistic electrons and that the density of sources of relativistic electrons decreases with radius. However, the unfavorable inclination and the rather large errors in the spectral indices at the boundaries of the galaxies do not permit a detailed modeling of the steepening of the radio spectrum with distance from the center. It is unclear whether the steepening is due to diffusion or convection in radial direction and/or in the direction perpendicular to the plane of the galaxies. The results for NGC 5055 and NGC 7331 indicate that the latter possibility can play a very important role. This is also suggested by observations of edge-on galaxies (Allen *et al.* 1978; de Bruyn and Hummel 1979) where the steepening of the radio spectrum predominantly occurs in the direction perpendicular to the plane of the galaxies.

REFERENCES

Allen, R. J. (1975). In *La Dynamique des Galaxies Spirales*, edited by L. Weliachew (CNRS, Paris), p. 157.

Allen, R. J., Baldwin, J. E., and Sancisi, R. (1978). Astron. Astrophys. **62**, 397.

Baars, J. W. M., and Hooghoudt, B. G. (1974). Astron. Astrophys. **31**, 323.

Bosma, A. (1978). Thesis, University of Groningen.

Brindle, C., French, D. K., and Osborne, J. L. (1978). Mon. Not. R. Astron. Soc. **184**, 283.

Brouw, W. N. (1971). Thesis, University of Leiden.

Casse, J. L., and Muller, C. A. (1974). Astron. Astrophys. **31**, 333.

de Bruyn, A. G., and Hummel, E. (1979). Astron. Astrophys. **73**, 196.

de Jong, M. L. (1966). Astrophys. J. **144**, 553.

de Jong, M. L. (1967). Astrophys. J. **150**, 1.

de Vaucouleurs, G., de Vancouleurs, A., and Corwin, H. G., Jr. (1976). *Second Reference Catalogue of Bright Galaxies* (University of Texas, Austin).

Ekers, R. D., Allen, R. J., and Luyten, J. R. (1973). Astron. Astrophys. **27**, 77.

Ekers, R. D., and Sancisi, R. (1977). Astron. Astrophys. **54**, 973.

Gallouët, L., Heidmann, N., and Dampierre, F. (1973). Astron. Astrophys. Suppl. **12**, 89.

Gioia, I. M., and Gregorini, L. (1980). Astron. Astrophys. Suppl. **41**, 329.

Heeschen, D. S., and Wade, C. M. (1964). Astron. J. **69**, 277.

Holmberg, E. (1958). Medd. Lund. Obs. II, No. 136.

Högbom, J. A. (1974). Astron. Astrophys. Suppl. **15**, 417.

Högbom, J. A., and Brouw, W. N. (1974). Astron. Astrophys. **33**, 289.

Hummel, E. (1980). Astron. Astrophys. Suppl. **41**, 151.

Hummel, E. (1981). Astron. Astrophys. **93**, 93.

Hummel, E., Sancisi, R., and Ekers, R. D. (1981). In preparation.

Israel, F. P., and van der Hulst, J. M. (1981). In preparation.

Klein, U., and Emerson, D. T. (1981). Astron. Astrophys. **94**, 29.

Moffet, A. T. (1975). In *Stars and Stellar Systems* (University of Chicago, Chicago), Vol. IX, p. 211.

Morgan, W. W. (1958). Publ. Astron. Soc. Pac. **70**, 364.

Nilson, P. (1973). *Uppsala General Catalog of Galaxies*, Uppsala Astron. Obs. Ann. **6**.

Protheroe, R. J., and Wolfendale, A. W. (1980). Astron. Astrophys. **92**, 175.

Rockstroh, J. M., and Webber, W. R. (1978). Astrophys. J. **224**, 677.

Schwarz, U. J. (1978). Astron. Astrophys. **64**, 345.

Segalovitz, A. (1977). Astron. Astrophys. **54**, 703.

van der Hulst, J. M. (1981). In preparation.

van der Kruit, P. C. (1973). Astron. Astrophys. **29**, 321; **29**, 249.

van der Kruit, P. C. (1977). Astron. Astrophys. **59**, 359.

van der Kruit, P. C. (1978). In *Structure and Properties of Nearby Galaxies*, IAU Symposium No. 77, edited by E. M. Berkhuijsen and R. Wielebinski (Reidel, Dordrecht), p. 33.

van der Kruit, P. C., Allen, R. J., and Rots, A. H. (1977). Astron. Astrophys. **55**, 421.

van Someren Gréve, H. W. (1974). Astron. Astrophys. Suppl. **15**, 343.